Current Biology 24, 2136–2141, September 22, 2014 ©2014 Elsevier Ltd All rights reserved http://dx.doi.org/10.1016/j.cub.2014.07.053

Report

Self-Generated Movements with "Unexpected" Sensory Consequences

Alexandre Tiriac,[1,2] Carlos Del Rio-Bermudez,[1] and Mark S. Blumberg[1,2,3,*]
[1]Department of Psychology
[2]Delta Center
[3]Department of Biology
University of Iowa, Iowa City, IA 52242, USA

Summary

The nervous systems of diverse species, including worms and humans, possess mechanisms for distinguishing between sensations arising from self-generated (i.e., expected) movements from those arising from other-generated (i.e., unexpected) movements [1–3]. To make this critical distinction, animals generate copies, or corollary discharges, of motor commands [4, 5]. Corollary discharge facilitates the selective gating of reafferent signals arising from self-generated movements, thereby enhancing detection of novel stimuli [6–10]. However, for a developing nervous system, such sensory gating would be counterproductive if it impedes transmission of the very activity upon which activity-dependent mechanisms depend [11]. In infant rats during active (or REM) sleep—a behavioral state that predominates in early infancy [12–16]—neural circuits within the brainstem [17, 18] trigger hundreds of thousands of myoclonic twitches each day [19]. The putative contribution of these self-generated movements to the activity-dependent development of the sensorimotor system is supported by the observation that reafference from twitching limbs reliably and substantially triggers brain activity [20–23]. In contrast, under identical testing conditions, even the most vigorous wake movements reliably fail to trigger reafferent brain activity [21–23]. One hypothesis that accounts for this paradox is that twitches, uniquely among self-generated movements, lack corollary discharge [23]. Here, we test this hypothesis in newborn rats by manipulating the degree to which self-generated movements are expected and, therefore, their presumed recruitment of corollary discharge. We show that twitches, although self-generated, are processed as if they are unexpected.

Results and Discussion

Recording Sensory Responses in the Primary Motor Cortex

Unanesthetized 8- to 10-day-old (P8–P10) rats (n = 11) cycled freely between sleep and wake while head-fixed in a stereotaxic apparatus with their limbs dangling freely (Figure 1A). We used 16-channel silicon electrodes to record extracellular neural activity from the hindlimb region of the primary motor cortex (M1). We chose to investigate M1 because, contrary to its designation as a motor structure, M1 also processes sensory (including proprioceptive) information [24], beginning early in development [25]. Also, because the cortical motor map develops gradually over the postnatal period, stimulation of M1 at early ages has a lower probability of producing a movement than in adults [26]. It must also be stressed that M1 appears to play no role in the production of twitches [17, 18]. For these reasons, we began this study with the primary aim of exploring the developmental foundations of sensorimotor processing within M1.

In pilot experiments, we established the coordinates of the hindlimb region of M1 using electrical stimulation to specifically elicit contralateral hindlimb movements. Then, for every pup tested here, we verified electrode location by manually stimulating the contralateral and ipsilateral hindlimbs, as well as both forelimbs and the tail, to confirm the specificity of M1 responding to the contralateral hindlimb (see Movie S1 available online); whereas flexing of the hindlimb effectively triggered M1 activity, tactile stimulation alone did not. Histology showed that electrodes were located in agranular cortex (Figure 1B, left).

The linear arrangement of the electrode sites (100 μm between sites) allowed for simultaneous recording from multiple cortical layers. Every other electrode site was filtered to identify spindle bursts in the local field potential (LFP; Figure 1B, right, blue traces) or multiunit activity (MUA; Figure 1B, right, black traces). All recorded units were located in the deep layers of M1. Spindle bursts were defined as described previously [20] (Figure 1B, blue highlight).

Twitch-Related, But Not Wake-Related, Movements Trigger M1 Activity

As shown in Figure 1C for a representative recording, both LFP and MUA activity in M1 occurred predominantly during periods of active sleep. This activity was particularly prominent during periods of hindlimb twitching (see Movie S1). In contrast, although wake-related hindlimb movements were frequent and vigorous, M1 activity was nearly absent (see Movie S1). Across all pups, there was a significant increase in mean rates of spindle bursts ($t_{10} = 9.2$, $p < 0.01$) and mean unit firing rates ($t_{16} = 3.2$, $p < 0.01$, n = 17 units, one to two units per pup) during sleep (Figure 1D). Moreover, LFP power and unit activity increased significantly after twitches with a latency of at least 100–125 ms (Figure 1E), consistent with previous reports of twitch-related reafference in the cerebral cortex [21, 22]. Finally, these results were replicated in P4 and P12 rats, demonstrating the stability of the effect across early development (Figure S1).

Hindlimb Exafference Triggers M1 Activity Regardless of State

It is possible that the data in Figure 1 resulted from global gating of all wake-related sensory input. If this is true, then manual stimulation of the hindlimb (i.e., exafference) should be able to trigger M1 activity during sleep, but not during wake. To rule out this possibility, we manually flexed the hindlimb contralateral to M1 as pups cycled between sleep and wake over a period of 10 min. Figure 2A depicts representative stimulations (arrows) performed during each state and the neural responses that follow these stimulations. Across all pups tested (n = 11), we observed significant increases in both LFP power and unit activity in response to stimulations regardless of behavioral state (Figure 2B). Importantly, because exafference was transmitted to M1 during periods

*Correspondence: mark-blumberg@uiowa.edu

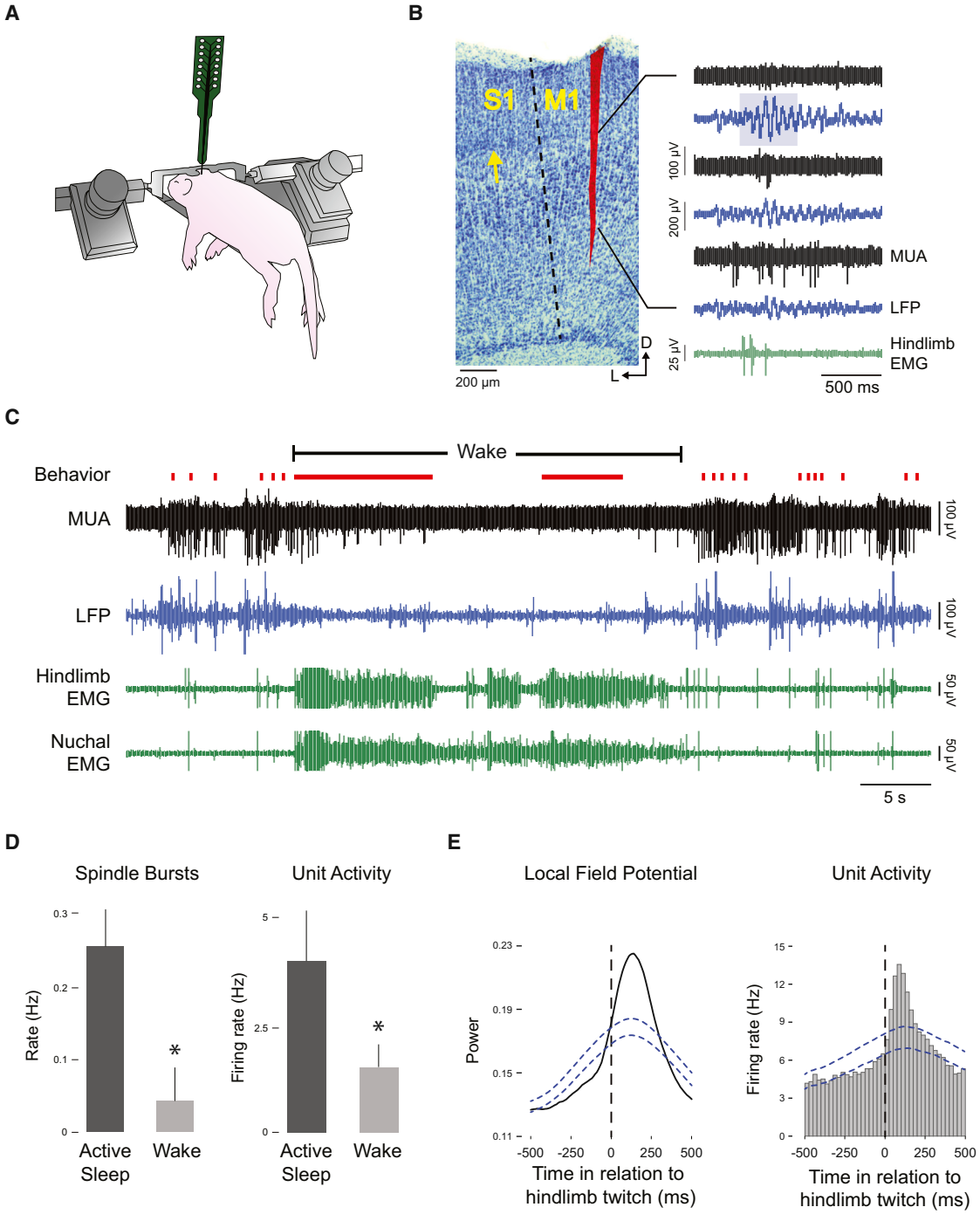

Figure 1. Hindlimb Twitches, but Not Wake-Related Hindlimb Movements, Trigger M1 Activity

(A) For these recordings, P8–P10 rats were head-fixed in a stereotaxic apparatus and maintained at thermoneutrality. The torso was supported by a platform, and the limbs dangled freely.

(B) Left: a coronal brain section, stained with cresyl violet, depicts the electrode track for a P10 subject. M1 is medial to the primary somatosensory cortex (S1) and is agranular; the granular cell layer in S1 is denoted by the arrow. Right: recordings from six sequential electrode sites with 100 μm separation. Signals are alternately filtered for multiunit activity (MUA; black traces) and local field potentials (LFP; blue traces). The spindle burst (blue highlighting) co-occurs with a burst of action potentials after a hindlimb twitch (green trace).

(C) Representative data depicting sleep and wake behavior, MUA, LFP, and hindlimb and nuchal electromyogram (EMG) during spontaneous sleep-wake cycling. Red tick marks denote hindlimb twitches, and red horizontal lines denote hindlimb wake movements.

(D) Mean (+SEM) rate of spindle burst (n = 11) and unit (n = 17) activity during active sleep and wake periods. *, significant difference from other group, $p < 0.05$.

(E) Waveform average and event correlation for LFP power and unit activity, respectively, in relation to hindlimb twitches for pooled data (4,047 and 6,358 twitches, respectively). The blue dashed lines denote upper and lower acceptance bands ($p < 0.05$).

See also Figures S1 and S2.

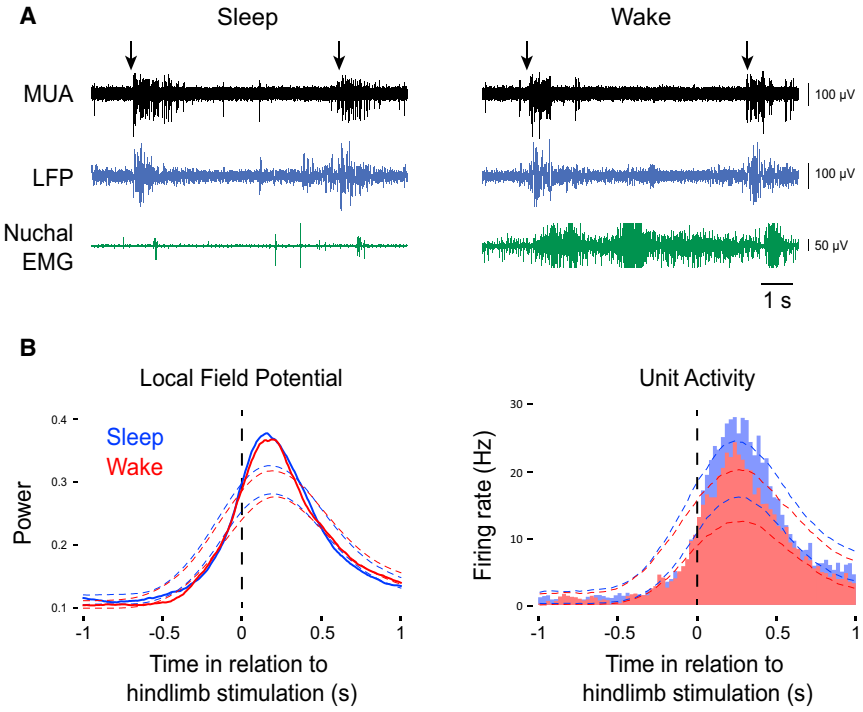

Figure 2. Exafferent Hindlimb Stimulation Triggers M1 Activity Regardless of Behavioral State

(A) Representative recordings in P8–P10 subjects depicting multiunit activity (MUA; black traces) and local field potential (LFP; blue traces) responses to hindlimb stimulation (arrows) during sleep (left) or wake (right). Nuchal EMG (green traces) is also shown.

(B) Left: waveform averages for LFP power in relation to hindlimb stimulation during sleep (blue line) and wake (red line) for data pooled across all subjects (n = 11). Thresholds for statistical significance are indicated by the color-coded dotted lines. Right: event correlations for unit activity in relation to hindlimb stimulation during sleep (blue histogram; 417 stimulations) and wake (red histogram; 418 stimulations) for data pooled across all units (n = 17). Color-coded dotted lines denote upper and lower acceptance bands ($p < 0.05$).

See also Figure S2.

of high muscle tone (see Figure 2A, right), muscle tone alone cannot account for the wake-related gating of reafference. Finally, there was no significant difference in maximum LFP power between sleep and wake ($t_{10} = 1.3$); in contrast, there was a small (<10%) but significant difference in maximum unit firing rate ($t_{16} = 4.1$, $p < 0.005$). In any event, it is clear that there is no global gating of sensory input to M1 during wake.

"Unexpected" Self-Generated Movements Trigger M1 Activity

By design, because pups' limbs dangled freely in the apparatus (see Figure 1A), there was no opportunity for unexpected reafference from hindlimb movements. Consequently, the lack of M1 activity after wake-related hindlimb movements is consistent with the idea that corollary discharge gates or cancels the expected reafference from self-generated movements [1, 3] (Figure S2A). In contrast, exafferent stimulation of the hindlimb cannot, by definition, be accompanied by corollary discharge and is therefore unexpected (Figure S2B), thus explaining the findings presented in Figure 2. We next evoked self-generated movements that differ in their expectancy so as to provide insight into the mechanisms by which twitches trigger M1 activity. If corollary discharge is involved in the processing of reafference from self-generated movements, we predicted that only unexpected movements (i.e., movements not accompanied by corollary discharge) would trigger M1 activity.

We first considered the possibility that with direct activation of lumbar spinal motoneurons we could trigger self-generated hindlimb movements while bypassing corollary discharge mechanisms that originate in the brain [27] (Figure S2C). In P8–P10 rats, we injected a nonselective 5-HT agonist, quipazine (3.0 mg/kg, intraperitoneal), which activates lumbar motoneurons and, as a consequence, produces limb movements [28] (see Movie S1). We recorded M1 activity before and after quipazine or saline injection (Figure 3A). Hindlimb movements, rate of spindle burst activity, and unit firing rate all increased significantly after quipazine administration. Specifically, for hindlimb movements, we found significant main effects of group ($F_{1,10} = 59.7$, $p < 0.001$) and time ($F_{1,10} = 184.8$, $p < 0.001$) and a significant group × time interaction ($F_{1,10} = 271.8$, $p < 0.001$; Figure 3B). For spindle bursts, we found significant main effects of group ($F_{1,10} = 24.5$, $p < 0.01$) and time ($F_{1,10} = 14.0$, $p < 0.01$) and a significant group × time interaction ($F_{1,10} = 29.2$, $p < 0.001$; Figure 3C). Finally, only four pups in each group yielded clear M1 units; nonetheless, for unit activity, we found a significant main effect of group ($F_{1,6} = 7.3$, $p < 0.05$), a nonsignificant main effect of time ($F_{1,6} = 4.8$, $p = 0.07$), and a marginally significant group × time interaction ($F_{1,6} = 5.9$, $p = 0.05$; Figure 3C). These results suggest that reafference from unexpected self-generated movements are conveyed to M1. They also suggest that spinal motoneurons and the associated local circuitry are downstream from the generators of corollary discharge that suppress reafference associated with wake-related limb movements.

Because quipazine was injected systemically, we wanted to ensure that the M1 activity we observed was due to effects on spinal motoneurons. Therefore, in two additional P8–P10 rats, we performed midthoracic spinal transections, thereby severing communication between the lumbar spinal cord and brain (Figure S3A). We immediately noticed that, consistent with previous findings in the somatosensory cortex after spinal transection [20], spindle bursts in M1 were much less prevalent (although not eliminated), thereby indicating that M1 activity is driven by limb reafference. Critically, injection of quipazine in the transected pups evoked hindlimb movements, similar to those in the nontransected pups (Figure S3B, top row). However, unlike in the nontransected pups, spindle burst activity in the transected pups did not increase after quipazine injection, thus suggesting that the earlier results arose from quipazine's direct effects on spinal circuits.

We next devised two behavioral methods that, although different in their presumed recruitment of corollary discharge mechanisms, allowed us to precisely trigger the onset of

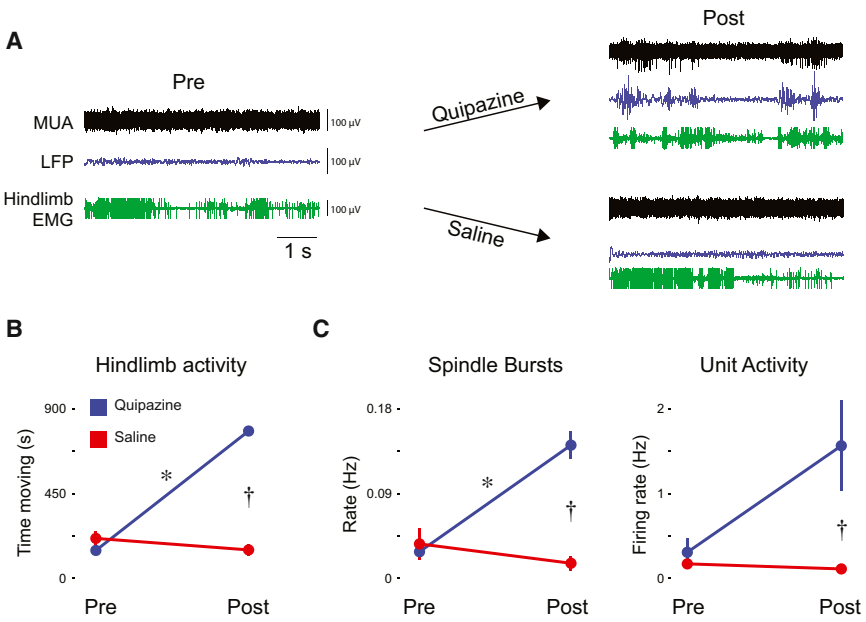

Figure 3. Pharmacological Induction of Hindlimb Movements Triggers M1 Activity

(A) Representative recordings in P8–P10 subjects depicting multiunit activity (MUA; black traces) and local field potentials (LFP; blue traces) before and after intraperitoneal injection of the serotonin agonist, quipazine, or saline. Hindlimb EMG (green traces) is also shown.

(B) Mean (±SEM) time that the hindlimb moved before and after quipazine or saline injection across all subjects (n = 6 per group).

(C) Mean (±SEM) rate of spindle burst (left; n = 6 per group) and unit (right; n = 4 per group) activity before and after quipazine or saline injection across all subjects. *, within-subjects significant difference, $p < 0.05$; †, between-subjects significant difference, $p < 0.05$.

See also Figures S2 and S3.

self-generated hindlimb movements. Moreover, because the two methods could be performed in the same subjects, we were able to directly assess differences in the processing of proprioceptive reafference arising from expected and unexpected movements. First, to produce unexpected reafference, we flicked the tail, thereby engaging local spinal circuits to cause reflexive hindlimb movements (Figure 4A, red trace; see also Figure S2C and Movie S1). Second, to produce expected reafference, we applied a cold stimulus to the snout [29], thereby causing brain-mediated arousal and associated activation of hindlimb movements (Figure 4A, blue trace; see also Figure S2A and Movie S1). Figure 4B presents representative data for the two manipulations. Both tail flick and application of the arousing stimulus (black arrows) elicited self-produced hindlimb movements (green arrows). As predicted, hindlimb movements elicited by tail flick, but not those elicited by the arousing stimulus, triggered significant increases in LFP power and unit activity in M1 (Figure 4C). Moreover, maximum values for both LFP and unit activity were significantly greater in response to tail flick than to the arousing stimulus (LFP: $t_5 = 4.1$, $p < 0.01$; MUA: $t_5 = 65.3$, $p < 0.001$).

To ensure that tail flicks did indeed activate local spinal circuitry, we performed tail flicks and arousing stimulations in the same two pups with midthoracic spinal transections described above. In the transected pups, flicks of the tail triggered hindlimb reflexes without affecting M1 LFP power (Figure S3B, bottom row). In contrast, stimulation of the snout was still able to arouse the transected pups (e.g., as seen by forelimb movements); however, as expected, we did not observe hindlimb movements or increases in M1 LFP power (data not shown).

Conclusions

The absence of M1 activity during self-generated wake-related movements, as observed here, is consistent with earlier reports describing differential sleep- and wake-related neural activity in the thalamus, somatosensory cortex, hippocampus, and cerebellum [21–23, 30]. This absence of M1 activity, coupled with the reliable activation of M1 by exafferent stimulation, suggests the operation of corollary discharge during wake-related movements (Figures S2A and S2B). Similarly, in primates, passive head movements drive neural activity in the vestibular nuclei, whereas active head movements do not, suggesting the selective cancelling of reafference by corollary discharge signals [31]. To further test the hypothesis that corollary discharge is functioning early in development, we manipulated the expectancy of the reafference from self-generated movements (Figure S2C). Only unexpected reafference reliably drove M1 activity, similar to what we observed with twitches (Figure S2D). To our knowledge, this is the first demonstration of a self-generated movement that is processed as if it were an other-generated movement and, therefore, unexpected.

Taken together, our results indicate that proprioceptors are sufficient to trigger the reafferent activity observed in M1. Recent evidence suggests that corollary discharge mechanisms originating in the brain suppress proprioceptive reafference from the hindlimbs that are processed by Clarke's column neurons [27]. At this time, however, little is known about the neural sources of twitches, especially early in development, thus preventing identification of the neural sources of corollary discharge or the sites where it modulates reafference. Therefore, an important next step is to determine whether the brainstem mechanisms that trigger twitches do not simultaneously generate corollary discharge or, alternatively, whether corollary discharge is generated but its effects are somehow inhibited. Regardless of the exact mechanism, the downstream effects on M1 activity would be the same.

Under normal waking conditions, corollary discharge makes it possible to account for expected reafferent signals triggered by one's own movements so that one is able to detect and respond appropriately to unexpected stimuli in the environment. Such accounting entails the gating or cancelling of reafference from self-generated movements. However, for the development and maintenance of precise, integrated, and hierarchically organized sensorimotor maps [32], infants likely depend upon the conveyance of high-fidelity sensory information from self-generated limb movements to developing brain structures [33, 34]. Twitch movements may be particularly well suited to this task because, unlike wake movements, they are produced discretely against a background of muscle atonia, both of which enhance signal-to-noise ratio [19]. Our results further suggest

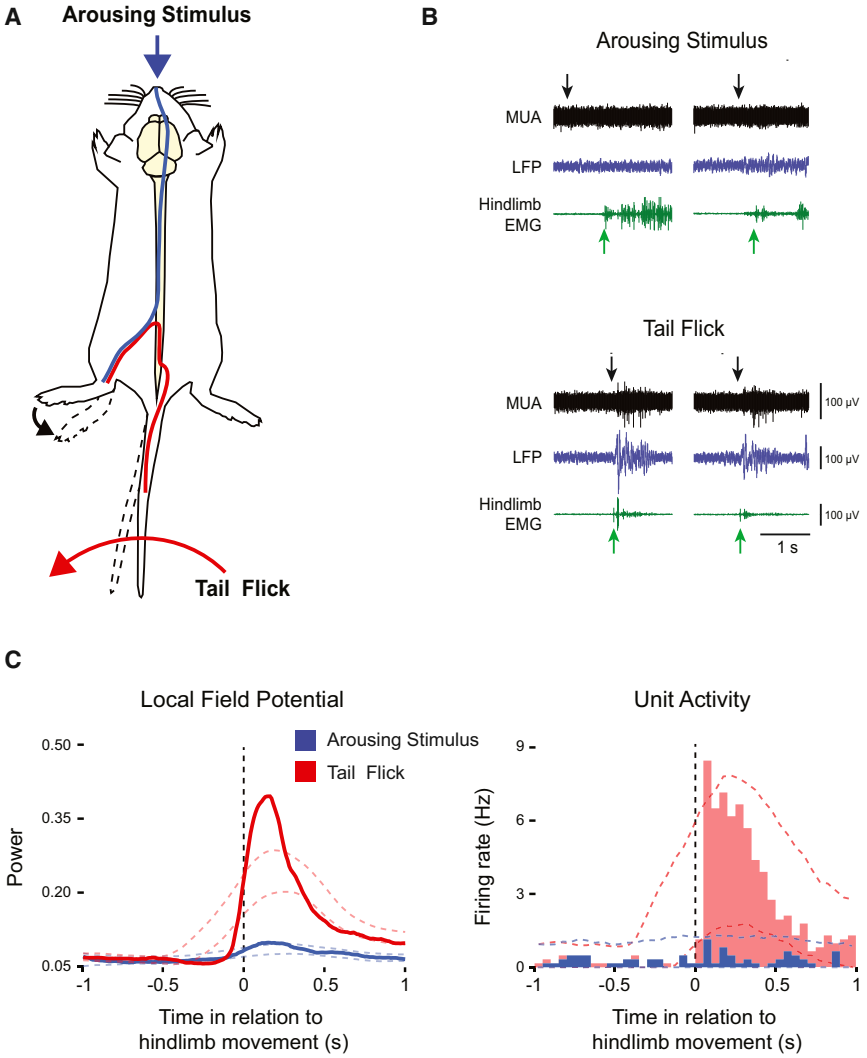

Figure 4. Effects of Expected and Unexpected Reafference on M1 Activity

(A) Schematic diagram representing the two types of self-generated movements. Application of a cold stimulus to the snout produced generalized arousal and elicited vigorous hindlimb movements, thereby producing expected reafference (blue pathway). A tail flick engaged local spinal circuits to cause a reflexive movement of the hindlimb, thereby producing unexpected reafference (red pathway).

(B) Representative recordings in P8–P10 subjects depicting multiunit activity (MUA; black traces) and local field potentials (LFP; blue traces) in response to the arousing stimulus (top) or tail flick (bottom). Black arrows denote stimulus presentation and green arrows denote onset of hindlimb activity.

(C) Waveform averages for LFP power (left) and event correlations for unit activity (right) in relation to onset of hindlimb movement for data pooled across all animals (n = 6) and units (n = 6), respectively (arousing stimulations = 102, tail flicks = 87). Color-coded dashed lines denote upper and lower acceptance bands ($p < 0.05$).

See also Figures S2 and S3.

that the high fidelity of twitching depends upon the suspension of corollary discharge mechanisms, providing the infant with ideal conditions for activity-dependent development of the spinal cord [35], cerebellum [23], and forebrain [20–22, 36]. The information provided by twitching limbs may also enable the construction and calibration of internal models and predictive codes, which are thought to be essential for flexible and efficient sensorimotor control throughout the lifespan [37–39].

Experimental Procedures

All experiments were approved by the Institutional Animal Care and Use Committee of The University of Iowa. The apparatus and methods for recording and analyzing neural and muscle activity in head-fixed pups have been described previously [18, 21, 22]. All surgeries were performed under isoflurane anesthesia, and data were collected from unanesthetized subjects; brain temperature was maintained at 36°C–37°C. As described previously [23], spike sorting was performed in Spike2 (Cambridge Electronic Design). Sleep and wake states were determined by analysis of the nuchal EMG in conjunction with behavioral scoring [18, 21, 22]. Active sleep was characterized by the occurrence of myoclonic twitches against a background of muscle atonia [40]. State-related differences in M1 activity were tested within each subject (Wilcoxon matched-pairs signed-ranks test) and across subjects (paired t test). Spikes of EMG activity with amplitudes greater than 3× baseline were considered twitches. For testing of the relations between events (e.g., twitches) and M1 activity, twitch-triggered event correlations and waveform averages were constructed [22]. We tested statistical significance for event correlations and waveform averages using a jitter protocol [41, 42] implemented in MATLAB (MathWorks). We corrected for multiple comparisons using the method of Amarasingham et al. [43]; this method produces upper and lower confidence bands for each event correlation and waveform average. ANOVA was used to evaluate the influence of quipazine administration on hindlimb movements, spindle bursts, and unit activity.

Supplemental Information

Supplemental Information includes Supplemental Experimental Procedures, three figures, and one movie and can be found with this article online at http://dx.doi.org/10.1016/j.cub.2014.07.053.

Author Contributions

A.T., C.D.R.-B., and M.S.B. designed the study, A.T. and C.D.R.-B. collected and analyzed the data, and A.T. and M.S.B. wrote the paper.

Acknowledgments

We are very grateful to Matthew Harrison for statistical assistance and to Adam Hantman, Kathleen Cullen, Robert Wurtz, Greta Sokoloff, and Karen Adolph for many helpful comments on the manuscript. This work was supported by a grant from the NIH (HD63071) to M.S.B. The Fulbright Foreign Student Program supported C.D.R.-B.

Received: June 11, 2014
Revised: July 19, 2014
Accepted: July 21, 2014
Published: August 14, 2014

References

1. Crapse, T.B., and Sommer, M.A. (2008). Corollary discharge across the animal kingdom. Nat. Rev. Neurosci. *9*, 587–600.
2. Poulet, J.F.A., and Hedwig, B. (2007). New insights into corollary discharges mediated by identified neural pathways. Trends Neurosci. *30*, 14–21.
3. Cullen, K.E. (2004). Sensory signals during active versus passive movement. Curr. Opin. Neurobiol. *14*, 698–706.
4. von Holst, E., and Mittelstaedt, H. (1950). The principle of reafference: interactions between the central nervous system and the peripheral organs. Naturwissenschaften *37*, 464–476.
5. Sperry, R.W. (1950). Neural basis of the spontaneous optokinetic response produced by visual inversion. J. Comp. Physiol. Psychol. *43*, 482–489.
6. Brooks, J.X., and Cullen, K.E. (2013). The primate cerebellum selectively encodes unexpected self-motion. Curr. Biol. *23*, 947–955.
7. Bell, C.C. (2001). Memory-based expectations in electrosensory systems. Curr. Opin. Neurobiol. *11*, 481–487.
8. Sommer, M.A., and Wurtz, R.H. (2002). A pathway in primate brain for internal monitoring of movements. Science *296*, 1480–1482.
9. Poulet, J.F., and Hedwig, B. (2006). The cellular basis of a corollary discharge. Science *311*, 518–522.
10. Kennedy, A., Wayne, G., Kaifosh, P., Alviña, K., Abbott, L.F., and Sawtell, N.B. (2014). A temporal basis for predicting the sensory consequences of motor commands in an electric fish. Nat. Neurosci. *17*, 416–422.
11. Kirkby, L.A., Sack, G.S., Firl, A., and Feller, M.B. (2013). A role for correlated spontaneous activity in the assembly of neural circuits. Neuron *80*, 1129–1144.
12. Roffwarg, H.P., Muzio, J.N., and Dement, W.C. (1966). Ontogenetic development of the human sleep-dream cycle. Science *152*, 604–619.
13. Jouvet-Mounier, D., Astic, L., and Lacote, D. (1970). Ontogenesis of the states of sleep in rat, cat, and guinea pig during the first postnatal month. Dev. Psychobiol. *2*, 216–239.
14. Thurber, A., Jha, S.K., Coleman, T., and Frank, M.G. (2008). A preliminary study of sleep ontogenesis in the ferret (Mustela putorius furo). Behav. Brain Res. *189*, 41–51.
15. Scriba, M.F., Ducrest, A.-L., Henry, I., Vyssotski, A.L., Rattenborg, N.C., and Roulin, A. (2013). Linking melanism to brain development: expression of a melanism-related gene in barn owl feather follicles covaries with sleep ontogeny. Front. Zool. *10*, 42.
16. Gramsbergen, A., Schwartze, P., and Prechtl, H.F.R. (1970). The postnatal development of behavioral states in the rat. Dev. Psychobiol. *3*, 267–280.
17. Kreider, J.C., and Blumberg, M.S. (2000). Mesopontine contribution to the expression of active 'twitch' sleep in decerebrate week-old rats. Brain Res. *872*, 149–159.
18. Karlsson, K.Æ., Gall, A.J., Mohns, E.J., Seelke, A.M.H., and Blumberg, M.S. (2005). The neural substrates of infant sleep in rats. PLoS Biol. *3*, e143.
19. Blumberg, M.S., Marques, H.G., and Iida, F. (2013). Twitching in sensorimotor development from sleeping rats to robots. Curr. Biol. *23*, R532–R537.
20. Khazipov, R., Sirota, A., Leinekugel, X., Holmes, G.L., Ben-Ari, Y., and Buzsáki, G. (2004). Early motor activity drives spindle bursts in the developing somatosensory cortex. Nature *432*, 758–761.
21. Tiriac, A., Uitermarkt, B.D., Fanning, A.S., Sokoloff, G., and Blumberg, M.S. (2012). Rapid whisker movements in sleeping newborn rats. Curr. Biol. *22*, 2075–2080.
22. Mohns, E.J., and Blumberg, M.S. (2010). Neocortical activation of the hippocampus during sleep in infant rats. J. Neurosci. *30*, 3438–3449.
23. Sokoloff, G., Uitermarkt, B.D., and Blumberg, M.S. (2014). REM sleep twitches rouse nascent cerebellar circuits: implications for sensorimotor development. Dev. Neurobiol. Published online March 28, 2014. http://dx.doi.org/10.1002/dneu.22177.
24. Hatsopoulos, N.G., and Suminski, A.J. (2011). Sensing with the motor cortex. Neuron *72*, 477–487.
25. An, S. (2013). Long-term potentiation and neural network activity in the neonatal rat cerebral cortex. PhD thesis (Mainz: University of Mainz).
26. Martin, J.H. (2005). The corticospinal system: from development to motor control. Neuroscientist *11*, 161–173.
27. Hantman, A.W., and Jessell, T.M. (2010). Clarke's column neurons as the focus of a corticospinal corollary circuit. Nat. Neurosci. *13*, 1233–1239.
28. Brumley, M.R., and Robinson, S.R. (2005). The serotonergic agonists quipazine, CGS-12066A, and α-methylserotonin alter motor activity and induce hindlimb stepping in the intact and spinal rat fetus. Behav. Neurosci. *119*, 821–833.
29. Todd, W.D., Gibson, J.L., Shaw, C.S., and Blumberg, M.S. (2010). Brainstem and hypothalamic regulation of sleep pressure and rebound in newborn rats. Behav. Neurosci. *124*, 69–78.
30. Mohns, E.J., and Blumberg, M.S. (2008). Synchronous bursts of neuronal activity in the developing hippocampus: modulation by active sleep and association with emerging gamma and theta rhythms. J. Neurosci. *28*, 10134–10144.
31. Roy, J.E., and Cullen, K.E. (2004). Dissociating self-generated from passively applied head motion: neural mechanisms in the vestibular nuclei. J. Neurosci. *24*, 2102–2111.
32. Kleinfeld, D.D., Berg, R.W.R., and O'Connor, S.M.S. (1999). Anatomical loops and their electrical dynamics in relation to whisking by rat. Somatosens. Mot. Res. *16*, 69–88.
33. Marques, H.G., Imtiaz, F., Iida, F., and Pfeifer, R. (2013). Self-organization of reflexive behavior from spontaneous motor activity. Biol. Cybern. *107*, 25–37.
34. Blumberg, M.S., Coleman, C.M., Gerth, A.I., and McMurray, B. (2013). Spatiotemporal structure of REM sleep twitching reveals developmental origins of motor synergies. Curr. Biol. *23*, 2100–2109.
35. Petersson, P., Waldenström, A., Fåhraeus, C., and Schouenborg, J. (2003). Spontaneous muscle twitches during sleep guide spinal self-organization. Nature *424*, 72–75.
36. McVea, D.A., Mohajerani, M.H., and Murphy, T.H. (2012). Voltage-sensitive dye imaging reveals dynamic spatiotemporal properties of cortical activity after spontaneous muscle twitches in the newborn rat. J. Neurosci. *32*, 10982–10994.
37. Wolpert, D.M., Miall, R.C., and Kawato, M. (1998). Internal models in the cerebellum. Trends Cogn. Sci. *2*, 338–347.
38. Shipp, S., Adams, R.A., and Friston, K.J. (2013). Reflections on agranular architecture: predictive coding in the motor cortex. Trends Neurosci. *36*, 706–716.
39. Frith, C.D., Blakemore, S.J., and Wolpert, D.M. (2000). Explaining the symptoms of schizophrenia: abnormalities in the awareness of action. Brain Res. Brain Res. Rev. *31*, 357–363.
40. Seelke, A.M.H., and Blumberg, M.S. (2008). The microstructure of active and quiet sleep as cortical delta activity emerges in infant rats. Sleep *31*, 691–699.
41. Amarasingham, A., Harrison, M.T., Hatsopoulos, N.G., and Geman, S. (2012). Conditional modeling and the jitter method of spike resampling. J. Neurophysiol. *107*, 517–531.
42. Harrison, M.T., and Geman, S. (2009). A rate and history-preserving resampling algorithm for neural spike trains. Neural Comput. *21*, 1244–1258.
43. Amarasingham, A., Harrison, M.T., and Hatsopoulos, N.G. (2011). Conditional modeling and the jitter method of spike re-sampling: supplement. arXiv, 0901.0633v2. http://arxiv.org/abs/1111.4296.

Current Biology, Volume *24*

Supplemental Information

Self-Generated Movements with "Unexpected" Sensory Consequences

Alexandre Tiriac, Carlos Del Rio-Bermudez, and Mark S. Blumberg

1. Supplemental Figures

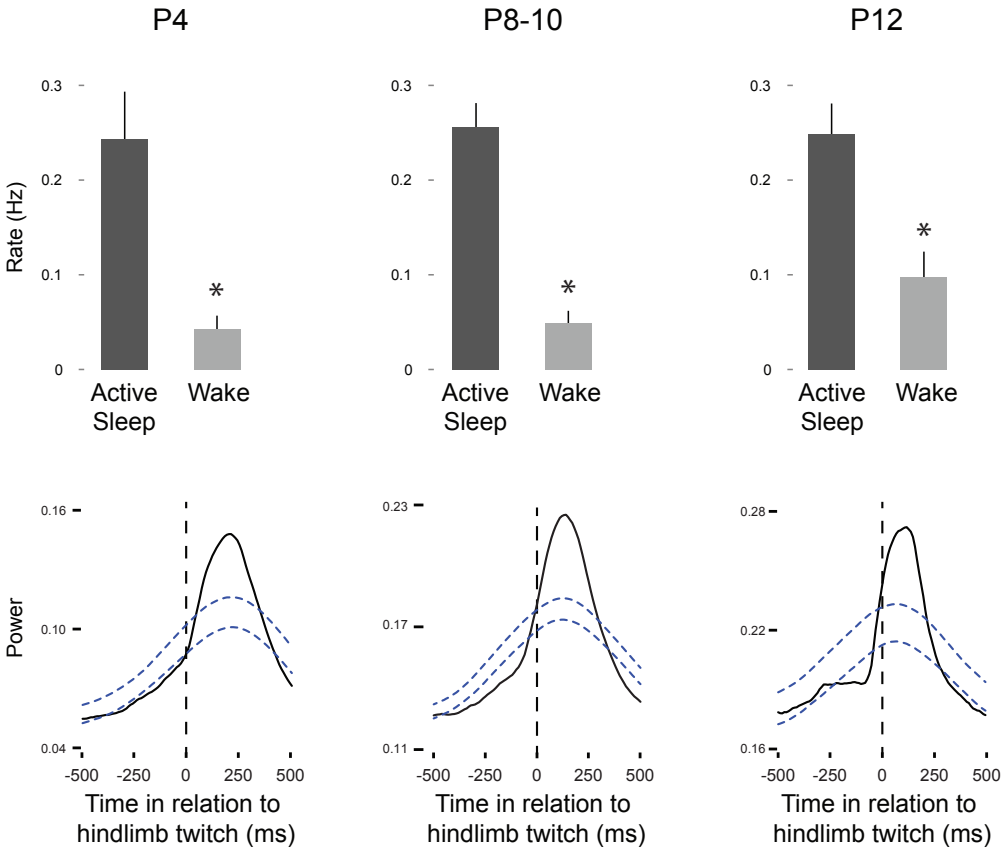

Figure S1, related to Figure 1. The hindlimb region of M1 exhibits more activity during active sleep than during wake across the early postnatal period in rats
Top row: Mean (+ SEM) rate of spindle bursts (P4: *n* = 6; P8-10: *n* = 11; P12: *n* = 6). * Significant difference from other group, *P* < .05. Bottom row: Waveform averages depicting occurrence of spindle bursts in relation to hindlimb twitches for data pooled across all subjects at each age (P4: 1172 twitches; P8-10: 4047 twitches; P12: 789 twitches). The blue dashed lines denote upper and lower acceptance bands (*P* < 0.05). The P8-10 data are the same as those presented in Figures 1D and 1E.

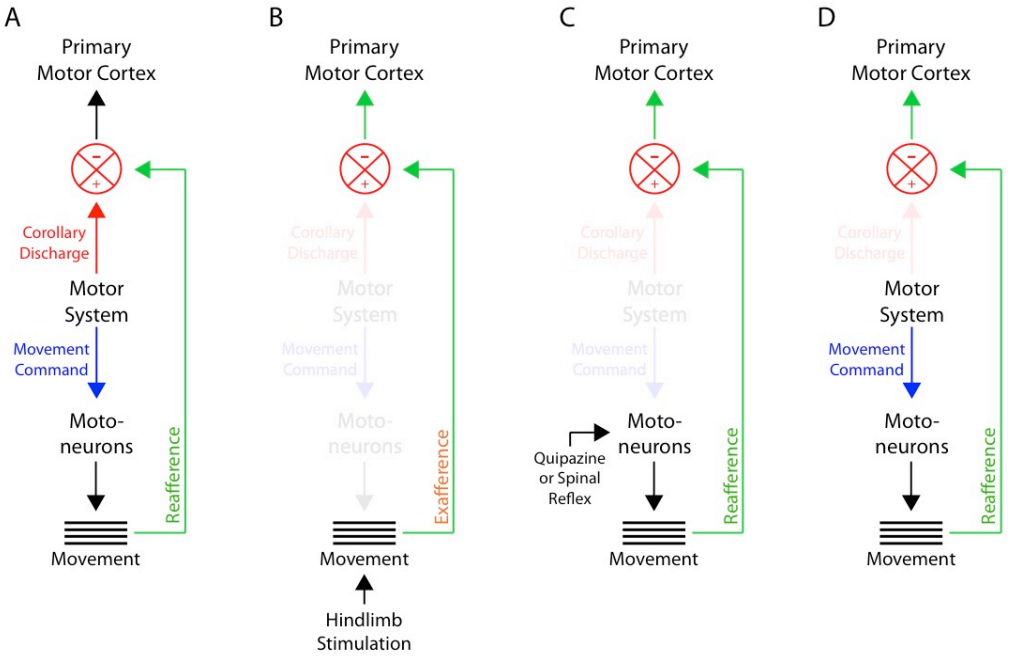

Figure S2, related to Figures 1-4. Schematic representation of the hypothetical mechanisms involved in conveying reafferent and exafferent signals to M1
(A) Conventional model depicting corollary discharge modulation of reafference for self-generated movements. Motor systems generate a descending movement command simultaneously with an ascending corollary discharge. Reafference from a moving limb is modulated by the corollary discharge signal before being conveyed to M1. When corollary discharge accurately predicts reafference, the signals can cancel each other out such that no signal is conveyed to M1, as observed here for waking movements. (B) Conventional model depicting exafference after hindlimb stimulation. No corollary discharge is generated because exafference is not self-produced. Thus, the exafference is conveyed to M1 without modification. (C) Model depicting two experimental manipulations used here to produce “unexpected” self-generated hindlimb movements. Both quipazine administration and local triggering of a spinal reflex are presumed to have produced their effects on hindlimb movements downstream of the corollary discharge mechanisms involved in modulating M1 activity. Thus, the reafferent signals are conveyed to M1 without modification. (D) Proposed model for the neural network involved in the production of twitches and the associated processing of reafference. According to this model, the brainstem mechanisms that trigger twitches do not generate corollary discharge or, alternatively, corollary discharge is generated but its effects are somehow inhibited. Regardless, reafference is conveyed to M1 in a fashion that is similar to exafference.

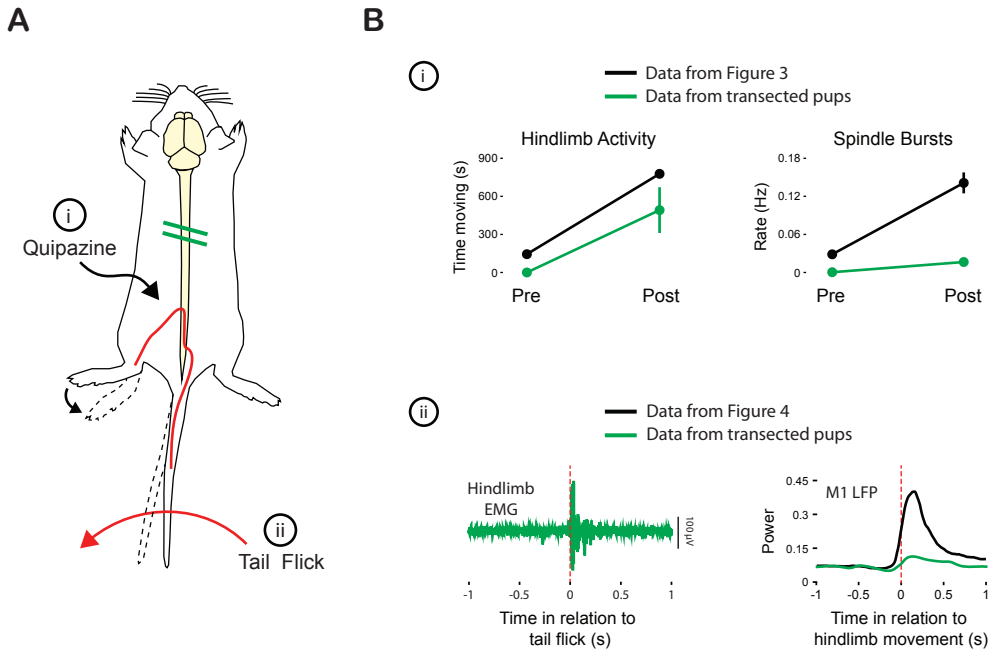

Figure S3, related to Figures 3-4. Effect of mid-thoracic spinal transection on hindlimb movements and M1 activity in response to (i) quipazine administration and (ii) tail flick

(A) Diagrammatic representation of the mid-thoracic transection and the two manipulations tested in P8-10 rats. (B) Top row: Mean (± SEM) time that the hindlimb moved and the rate of spindle burst production in M1 before and after quipazine administration for data presented in Figure 3 (*n* = 6, black lines) and spinally transected pups (*n* = 2, green lines). Bottom row: Waveform averages depicting hindlimb EMG activity in the transected pups associated with the onset of reflexive hindlimb movements triggered by tail flicks. The waveform average at right compares M1 LFP activity associated with the onset of reflexive hindlimb movements triggered by tail flicks for pooled data presented in Figure 4 (*n* = 6, black lines; 87 hindlimb movements) and spinally transected pups (*n* = 2, green lines; 21 hindlimb movements).

2. Supplemental Experimental Procedures

All experiments were carried out in accordance with the National Institutes of Health Guide for the Care and Use of Laboratory Animals (NIH Publication No. 80-23) and were approved by the Institutional Animal Care and Use Committee of the University of Iowa.

Subjects

A total of 44 Sprague-Dawley Norway rats (*Rattus norvegicus*) were used between the ages of 4 and 12 days of age. Males and females were used and littermates were always assigned to different experimental groups. Litters were culled to 8 pups within 3 days of birth. Mothers and their litters were housed in standard laboratory cages (48 x 20 x 26 cm). Food and water were available *ad libitum*. All animals were maintained on a 12:12 light-dark schedule with lights on at 0700 h.

Surgery

Head-fix preparation. For all studies, pups were prepared for testing using methods similar to those described previously [S1-3]. Under isoflurane anesthesia, bipolar electrodes (50 µm diameter; California Fine Wire, Grover Beach, CA) were implanted into the *extensor digitorum longus* muscle of the hindlimb and the nuchal muscle. The skin overlying the skull was removed and a custom-built head-fix apparatus was attached to the skull with cyanoacrylate adhesive. A small hole was drilled over the hindlimb region of primary motor cortex (M1; coordinates in relation to bregma: AP: -1.5 mm, L: 0.5 mm). In preliminary experiments, it was determined that electrical stimulation at this location of M1 produces movements of the contralateral hindlimb. After surgery, the pup was transferred to a humidified incubator maintained at thermoneutrality (35^{o}C) to recover for at least 1 hour, after which it was transferred to a stereotaxic apparatus. The pup's torso was supported on a narrow platform such that the limbs dangled freely on both sides. The pup acclimated for at least 1 additional hour before recordings began, by which time it was cycling between clear periods of sleep and wake.

Experimental Procedures

The EMG electrodes were connected to a differential amplifier (A-M Systems, Carlsborg, WA; amplification: 10,000x; filter setting: 300-5000 Hz). To record from motor cortex, 16-channel silicon depth electrodes (100 µm vertical separation; NeuroNexus, Ann Arbor, MI), with impedances ranging from 1-4 MΩ, were connected to a headstage and data acquisition system (Tucker-Davis Technologies, Alachua, FL) that amplified (10,000x) and filtered the signals. Of the 16 channels, every other one was filtered for local field potentials (LFPs) or multi-unit activity (MUA). To record LFPs, the signals were filtered using a 1-40 Hz band-pass. For MUAs, the signals were filtered using a 500-5000 Hz band-pass. A 60 Hz notch filter was also used. Neurophysiological and EMG signals were sampled at 12.5 kHz and 1 kHz, respectively, using a digital interface and Spike2 software (Cambridge Electronic Design, Cambridge, UK).

Prior to insertion of the silicon probe, the electrode surface was coated with fluorescent DiI (Life Technologies, Carlsbad, CA) for subsequent histological verification of electrode placement. A Ag/AgCl ground electrode (Medwire, Mt. Vernon, NY, 0.25

mm diameter) was placed into the visual cortex ipsilateral to the silicon probe. Brain temperature was monitored using a fine-wire thermocouple (Omega Engineering, Stamford, CT) placed in the visual cortex contralateral to the ground wire. For all experiments, brain temperature was maintained at 36-37˚C.

The electrode was positioned above motor cortex and was lowered to a depth of 0.5-1.0 mm. Electrode position was set once it was possible to reliably evoke neural activity by gentle stimulation of the contralateral hindlimb. Using procedures similar to those described previously [S1-3], data acquisition began after LFP signals were identified and had stabilized for at least 10 min; we also sought to record MUA activity but this was not always possible, especially at the younger ages. Recording sessions comprised continuous collection of neurophysiological and EMG data for at least 30 min. During acquisition, an experimenter monitored the subject's behavior and digitally marked the occurrence of sleep-related twitching and wake movements in synchrony with the physiological data. As described elsewhere [S1], myoclonic twitches are phasic, rapid, and independent movements of the limbs and tail against a background of muscle atonia; in contrast, wake movements, which are high-amplitude, coordinated movements occurring against a background of high muscle tone, include locomotion, stretching, and yawning. Finally, the experimenter was always blind to the physiological data when scoring behavior.

Experimental Manipulations

Hindlimb stimulation. For each pup, the hindlimb contralateral to the recording site was stimulated using a fine paintbrush over a period of 10 min. The brush was applied to the base of the paw and the limb was flexed at the knee. The stimulations were performed similarly during sleep and wake. On average, stimulations occurred every 5-10 s.

Pharmacological activation of hindlimb movements with quipazine. In 12 head-fixed P8-10 rats, M1 activity was recorded during a 15-min baseline period ("pre"). At the end of this baseline period, pups received a 0.1 ml intraperitoneal injection of the serotonin agonist, quipazine (Sigma-Aldrich, St. Louis, MO; dose: 3.0 mg/kg), or physiological saline (N=6 in each group). Five min after injection, M1 activity was recorded for an additional 15 min ("post").

Stimulation-induced triggering of hindlimb activity. In six head-fixed P8-10 rats, M1 activity was recorded in response to two types of stimulation, each designed to produce hindlimb movements via a different mechanism. First, to produce hindlimb activity via generalized arousal, a cold spatula was applied to the pup's snout [S4]. Second, to produce hindlimb activity via a local spinal circuit, the experimenter flicked the pup's tail. Both types of stimulation were presented during wake, within 2 s of a wake movement and while nuchal muscle tone remained elevated. When a stimulus was applied, the experimenter marked the event on the computer keyboard. The two types of stimulation were presented 15 times each in an intermixed, randomized order, with an inter-stimulation interval of at least one min. A stimulation was deemed successful if it elicited a hindlimb movement; on those rare occasions when a stimulation was not successful, that trial was not counted toward the total of 15 and was not included in the data analysis.

Mid-thoracic spinal transection. In two P8-10 rats under isoflurane anesthesia, the skin above the mid-thoracic spinal cord was cut. The brown adipose tissue was

gently peeled back to expose the vertebral column. At T8-T9, a blunt forceps was used to expose the spinal cord, which was then completely cut using fine scissors. The brown adipose tissue was replaced and the incision was closed using Vetbond (3M, Maplewood, MN). Each pup was then head-fixed and prepared for M1 recording as already described. For these pups, the methods used for testing were identical to those described above for general arousal and tail flick. After this protocol was complete, the pups were then injected with quipazine, again using the same methods as those described above.

Histology

At the end of each experiment, the pup was overdosed with sodium pentobarbital (1.5 mg/g) and perfused transcardially with phosphate buffered saline followed by 4% paraformaldehyde. Brains were sectioned at 50 μm using a freezing microtome (Leica Microsystems, Buffalo Grove, IL). Recording sites were verified by visualizing the DiI tract at 5-10X magnification using a fluorescent Leica microscope (Leica Microsystems, Buffalo Grove, IL). Tissue slices were then stained using cresyl violet and the location of the recording site was identified. For the two additional animals with spinal transections, the spinal cord was visualized using a surgical microscope and the completeness of the transection was confirmed.

Data Analysis

Spike sorting and spindle burst analysis. As described previously [S5], spike sorting was performed in Spike2 (Cambridge Electronic Design, Cambridge, UK). Spindle bursts were defined as comprising at least 3 oscillations, a dominant frequency of 10-15 Hz, and a duration of at least 100 ms [S6]. To aid in the identification of spindle bursts, the LFP channels were filtered using a 50 Hz low-pass filter. Next, the channel was converted using root mean square (RMS) with a time constant of 0.1 s. Five high-amplitude spindle bursts were averaged and the baseline value of the RMS channel was calculated. The midpoint between those two values was used as a threshold for identification of spindle bursts. A second pass through the data was performed to manually remove any spindle bursts that did not match the requisite criteria. Throughout this process, artifacts in the LFP and MUA signals were identified and manually removed.

Identification of behavioral state. Sleep and wake periods were defined using methods described previously [S1-3]. Briefly, the nuchal EMG signal was dichotomized into periods of high tone (indicative of wake) and atonia (indicative of sleep). Moreover, active sleep was characterized by the occurrence of myoclonic twitches against a background of muscle atonia [S7]. Spikes of EMG activity with amplitudes greater than 3x baseline were considered twitches.

Analysis of state-dependency. The mean rates of spindle burst production and unit activity were determined for each bout of wake and active sleep for each pup (there were at least 20 bouts of wake and active sleep for each pup). First, for each pup individually, successive bouts of wake and active sleep were treated as pairs and the Wilcoxon matched-pairs signed-ranks test (SPSS, IBM, Armonk, NY) was used to test for differences in rates of spindle burst production and unit activity between the two states. Although these data are not presented here, these rates were always

significantly higher during active sleep than during wake. Second, the mean rates of spindle burst production and unit activity during wake and active sleep were calculated for each pup and compared within each age group using paired *t* tests.

Event correlations and waveform averages. The relationship between twitches and M1 activity was assessed as follows: First, the data for all pups within each age or experimental group were concatenated into one file. From this file, using twitches as triggers, event correlations (composed of 40 25-ms bins) of unit activity and waveform averages of spindle activity were constructed using a 1-s window. We tested statistical significance for both event correlations and waveform averages by jittering twitch events 1000 times within a 500-ms window using the interval jitter parameter settings within PatternJitter [S8, 9] implemented in Matlab (MathWorks, Natick, MA). We corrected for multiple comparisons using the method of Amarasingham et al. [S10]; this method produces upper and lower confidence bands for each event correlation and waveform average.

Differences in LFP power between experimental conditions were tested by first determining, for each pup, maximum power within the 1-s window. Similarly, differences in unit activity were tested by first determining, for each unit, the maximum firing rate over all 40 bins within the 1-s window. Paired *t* tests were then used to assess statistical significance.

Stimulus-triggered event correlations and waveform averages. The 10-min recordings from the hindlimb stimulation trials were divided into periods of sleep and wake. Event correlations (for unit activity; composed of 80 25-ms bins) and waveform averages (for LFPs) were constructed using a 2-s window and hindlimb stimulation as the trigger. We tested statistical significance using the jittering method described above.

For the experiment comprising application of a cold spatula to the snout (i.e., general arousal) and tail flick (i.e., spinally generated reflex), the first hindlimb movement (as determined using EMG) within 3 seconds of the presentation of a stimulus was marked as an event. These events were next collected into two groups (i.e., general arousal and spinal reflex). Finally, event correlations (for unit activity) and waveform averages (for LFPs) were constructed and statistical significance was determined using the jittering method.

Pharmacological activation of hindlimb movements with quipazine. For each pup in the 15 min before and after quipazine or saline administration, periods of active wake were identified when muscle tone was high and continuous limb movements were observed. The total amount of time that the contralateral hindlimb was moving, the number of spindle bursts, and the number of action potentials were quantified. To evaluate the influence of quipazine administration on hindlimb movements, spindle bursts, and unit activity, we performed a 2 x 2 repeated-measures factorial ANOVA (SPSS, IBM, Armonk, NY). The pharmacological condition (quipazine or saline) served as the between-subjects factor and time (pre- or post-injection) as the repeated-measures factor.

For all tests, alpha was set to 0.05.

3. Supplemental References

S1. Karlsson, K. Æ., Gall, A. J., Mohns, E. J., Seelke, A. M. H., and Blumberg, M. S. (2005). The neural substrates of infant sleep in rats. PLoS Biol. *3*, e143.

S2. Mohns, E. J., and Blumberg, M. S. (2010). Neocortical activation of the hippocampus during sleep in newborn rats. J. Neurosci. *30*, 3438–3449.

S3. Tiriac, A., Uitermarkt, B. D., Fanning, A. S., Sokoloff, G., and Blumberg, M. S. (2012). Rapid whisker movements in sleeping newborn rats. Curr. Biol. *22*, 2075–2080.

S4. Todd, W. D., Gibson, J., Shaw, C., and Blumberg, M. S. (2010). Brainstem and hypothalamic regulation of sleep pressure and rebound in newborn rats. Behav. Neurosci. *124*, 69–78.

S5. Sokoloff, G., Uitermarkt, B. D., and Blumberg, M. S. (2014). REM sleep twitches rouse nascent cerebellar circuits: Implications for sensorimotor development. Dev. Neurobiol. doi: 10.1002/dneu.22177.

S6. Khazipov, R., Sirota, A., Leinekugel, X., Holmes, G. L., Ben-Ari, Y., and Buzsáki, G. (2004). Early motor activity drives spindle bursts in the developing somatosensory cortex. Nature *432*, 758–761.

S7. Seelke, A. M. H., and Blumberg, M. S. (2008). The microstructure of active and quiet sleep as cortical delta activity emerges in infant rats. Sleep *31*, 691–699.

S8. Amarasingham, A., Harrison, M. T., Hatsopoulos, N. G., and Geman, S. (2012). Conditional modeling and the jitter method of spike resampling. J. Neurophysiol. *107*, 517–531.

S9. Harrison, M. T., and Geman, S. (2009). A rate and history-preserving resampling algorithm for neural spike trains. Neural Comput. *21*, 1244–1258.

S10. Amarasingham, A., Harrison, M. T., and Hatsopoulos, N. G. (2011). Conditional modeling and the jitter method of spike re-sampling: Supplement. arXiv. Available at: http://arxiv.org/abs/1111.4296.